Malaysian Journal of Mathematical Sciences 17(3): 349–361 (2023)
https://doi.org/10.47836/mjms.17.3.07

Malaysian Journal of Mathematical Sciences

Journal homepage: https://mjms.upm.edu.my

Exact Analysis of Unsteady Solute Dispersion in Blood Flow: A Theoretical Study

Abidin, S. N. A. M.*[1], Jaafar, N. A.[1], and Ismail, Z.[1]

[1]*Department of Mathematical Sciences, Faculty of Science, Universiti Teknologi Malaysia, 81310 Johor Bahru, Johor, Malaysia*

E-mail: zuhaila@utm.my
**Corresponding author*

Received: 26 January 2023
Accepted: 14 July 2023

Abstract

The diameter of an artery can narrow due to atherosclerosis or stenosis, making it challenging to resolve solute dispersion issues as blood flows via a stenosed artery. The stenosis occurrence restricted drug dispersion and blood flow. This research introduces the establishment of a mathematical model in examining the unsteady dispersion with respect to the solute in overlapping stenosis arteries depicting blood as a Herschel-Bulkley (H-B) fluid model. Note that fluid velocity was obtained by analytically solving the governing and constitutive equations. The transport equation has been solved by employing a generalised dispersion model (GDM), in which the dispersion process is described. Accordingly, yield stress, stenosis height, slug input of solute length, as well as a rise in the power-law index have improved the peak with regard to the mean concentration and solute concentration. The maximum mean concentration yielded the effective dose for therapeutic concentration. In conclusion, this study is relevant to disease arteries, coagulating hemodynamics and may help physiologists in furnishing a more refined understanding of diffusion processes in cardiovascular hydrodynamics. An interesting application related to the present study is the transportation of drugs in the arterial blood flow.

Keywords: blood flow; solute; dispersion; Herschel-Bulkley fluid; mean concentration.

1 Introduction

The World Health Organization (WHO) reports cardiovascular disease (CVD), which accounts for 17% of all fatalities in 2022, is the leading cause of death worldwide. Atherosclerosis, commonly referred to as stenosis, is the primary cause of CVD. Recently, Hepatitis B and Coronavirus (COVID-19) have been considered the most common factors which increase the risk factors for atherosclerosis or stenosis [13]. Low-density lipoproteins, cellular waste products, cholesterol, calcium, fibrin as well as other substances gradually accumulate on the artery wall to induce stenosis [9, 33]. Such accumulation in the artery might decrease its cross-sectional area, which makes it difficult for blood to pass through. This results in inadequate blood flow to the heart [22]. Death might result from artery stenosis if it continues to deteriorate over time [18]. Additionally, the flow behaviour in the stenosed artery differs from normal arteries. Furthermore, stresses as well as resistance to flow is much greater in stenosed arteries when compared to the normal ones [33]. Therefore, understanding circulatory disorders can be improved by examining blood flow in a restricted artery. Damaged and blocked arteries are severe illnesses that affect a large number of people worldwide. We take the issue into consideration because of its significance, negative effects on society, and the need for additional research to deepen our understanding of the issue. Hence, it is crucial to comprehend the behaviour of blood flow in a stenotic artery because it differs greatly from blood flow in a healthy artery [12].

The stenosis geometry affects the blood movement across the artery. The stenosed artery depends on the stenosis shape, length, and height. Hence, a mathematical study of such a situation is significant. Numerous research has been conducted concerning the onset of sclerosis, and the majority of them classified the shape of the stenosis as either symmetric or asymmetric [27]. However, it is recognized that the stenosis could be numerous in nature or develop irregularly. Hossain and Haque [17] stated that overlapping stenosis has caused more CVDs than the single stenosed artery. Prashantha and Anish [23] agreed with [17] by highlighting that around 70 to 80% of CVDs occur in geometries which are complex such as in an overlapping stenosed artery. According to Freidoonimehr et al. [14], the shape as well as the degree of stenosis of a stenotic coronary artery have crucial impacts on the arterial blockage. Uddin et al. [35] in their study stated that stenosis effect on blood flow might lead to severe arterial diseases and can be useful in medical science. Recently, Mehkheimer et al. [20], using an overlapped stenotic artery, studied the mixing of blood with synovial fluid application to nanoparticle drug delivery. Riahi and Origaza [24] investigated the solute transport in a constricted porous artery consisting of an overlapping stenosis. Apart from that, via an overlapping stenosed artery with a porous wall, Dada et al. [11] examined a double-layered blood flow. Here, an overlapped stenotic artery was extensively studied [30, 37].

Transportation of solute (drugs) in arterial blood flow with stenosis is an intriguing application of the current study. When a drug is being injected into an artery, it becomes crucial to determine the drug concentration at a later site in the field of arterial pharmacokinetics. Until a certain extent, the efficacy is effectively therapeutic; however, at that point, it starts to develop local or systemic toxicity, which can have catastrophic consequences. Specifically, as a result of diffusive as well as convective mechanisms in physiological systems, solutes such as nutrients, metabolic products, and drugs are carried by blood flow. The first significant study on dispersion was initiated by Taylor [32]. The author conducted experimental and theoretical studies of the solute's dispersion in a straight tube moving at a mean velocity. He was the first scientist to introduce the concept of axial dispersion. In the study, the author discovered that combining molecular diffusion as well as the mean velocity yields the diffusion of the solute at a molecular diffusivity given by $D_{eff} = a^2 {w_m}^2/48\ D_m$, in which D_m represents the molecular diffusivity, a denotes the tube radius, while w_m depicts the mean axial velocity. Meanwhile, Aris [4] executed the moment method and reported that Taylor's dispersion theory could only be valid provided that

$D_{eff} \geq D_m$. In order to improve Taylor's dispersion theory, Aris [4] included the axial molecular diffusion effect, $D_{eff} = D_m + a^2 {w_m}^2/48\, D_m$ and the combination of both findings were described as the Taylor-Aris's dispersion theory. Nevertheless, the proposed theory was inappropriate for short durations despite being valid for a prolonged period. Subsequently, Gill and Sankarasubramanian [16] offered an alternative method called the generalised dispersion model (GDM) to generate a consistent, accurate solution to the transport equation. This approach explains how a solute disperses throughout the bloodstream.

Solute transport has been achieved through a number of mechanisms which include convection as well as axial diffusion. According to Debnath et al. [7] the solute transport mechanism present in Newtonian blood flow was discussed using the GDM method, in which the solute is absorbed by the capillary wall with a linear irreversible reaction rate. In addition, Roy and Beg [25] and Roy and Shaw [26] imposed a GDM method to solve the convection-diffusion equation in a two-fluid model to get the transport coefficients and mean concentration of solute. Additionally, the latter is different from the former due to the permeability of the vessel wall as well as the type of fluid. Furthermore, the stenosis severity as well as geometry have an important influence on the distribution of mass concentration as stated by [3]. Numerous recent studies used GDM to govern solute transport in the blood flow [2, 6]. Not all fluids behave in advanced engineering in the same way as Newtonian fluids. Since their nonlinear shear rate as well as stress relationship, non-Newtonian fluids attract the attention of numerous researchers and have a big range of applications in industry and biology, including enhanced oil recovery, chemical processes like those found in distillation towers and fixed-bed reactors, and the use of pumping fluids like colloidal fluids, liquid crystals, synthetic lubricants, and biofluids (animal and human blood) [15, 1]. Despite the use of Newtonian and a number of non-Newtonian fluid models to explore blood motion, it is now understood that the Herschel-Bulkley (H-B) model best captures the behaviour of blood. Furthermore, a type of non-Newtonian fluid known as H-B fluids must experience finite critical stress, or yield stress, to deform. Additionally, these materials act as rigid solids when the local shear is less than the yield stress. Moreover, the material flows with a nonlinear stress-strain relationship once the yield stress is exceeded, either as a shear-thickening fluid or as a shear-thinning fluid. Paints, cement, food goods, polymers, slurries, blood flow, and pharmaceutical products are a few examples of fluids that behave in this manner [29].

Sankar et al. [28] used H-B fluid in poiseuille flow to study the effects of geometrical as well as fluid parameters in the medium which are porous. Wajihah and Sankar [36] emphasized that blood is a complex fluid with non-Newtonian properties, shear thinning behavior, viscoplasticity (yield stress), and a thixotropic nature in their review. Singh and Murthy [31] investigated pulsatile H-B fluid flow with unsteady solute dispersion in a tube to assess the impact of skewness and kurtosis on the distribution and its concentration. According to Tiwari et al. [34], variations in blood viscosity explained the unsteady solute dispersion using H-B fluid. They explained how an enhancement in the viscosity index impacts the diffusion coefficients and fluid flow velocity. In the following year, Chauhan and Tiwari [10] used Jeffrey fluid and H-B fluid to understand the solute dispersion through microvessels with absorbing walls under varying viscosity assumptions.

As a result, investigations on the issue of solute dispersion in blood flow with the inclusion of a mass transfer in an artery having stenosis are lacking, according to earlier publications in the literature. Therefore, it is essential to investigate solute dispersion in a non-Newtonian fluid in order to get accurate results that more accurately depict physical issues. To comprehend how non-Newtonian rheology affects solute dispersion, it is also vital to grasp the rheological parameters. This issue can be resolved by forecasting the mean concentration of solute and the transport coefficients in narrow arteries with low shear rates. For axisymmetric, incompressible, as well as fully developed flow of blood in a rigid, impermeable artery with constant axial pressure gradient and viscosity, a novel mathematical model is created in the present study. Hence, combining

many features that have only been examined separately in prior studies constitutes the novelty of the present research. Herein we amalgamate (i) a non-Newtonian fluid model consisting of overlapping stenosis as well as (ii) the GDM to solve the convection-diffusion equation. The current issue takes into account solute or drug distribution in stenosed arterial blood flow, in which a H-B fluid model has been taken into consideration. Knowing how a drug is capable of being distributed, how its amount varies along an artery, and, in particular, how atherosclerosis can affect the amount of drug that is needed in order to reach its target for the patient's specific illness is important for understanding the problem faced when transporting the drug to a patient whose artery has been damaged resulting from the occurrence of atherosclerosis. We discover, in particular, that drug diffusivity has a significant impact on drug transport and that faster drug delivery is achieved with smaller values of the diffusivity coefficient when the initial drug value is not too small. The research findings will improve the existing knowledge of several physiological processes that involve introducing and transporting a known amount of solutes, such as drugs, into the bloodstream in the presence of stenosis. In the field of arterial pharmacokinetics, when a drug is injected into an artery, it is essential to assess the drug concentration at some downstream site. The injected drug has therapeutic efficacy up to a certain point, after which it develops systemic toxicity, which can have serious implications. The study has credible applications in medicine and biomedical engineering. In addition, the outcomes of the present work help in the treatment of many cardiovascular diseases. Therefore, this research may aid doctors in determining the extent of stenosis and its long-term effects or in the treatment of cardiovascular ailments including myocardial infarction, stroke, and heart attacks. In the event of more severe stenosis, this investigation may be furthered by the addition of other rheological and physical data.

2 Mathematical Formulation and Solution Methodology

The flow of a steady non-Newtonian fluid that is incompressible through a circular artery with overlapping stenosis, as depicted in Figure 1, is taken into consideration. It is unidirectional, laminar, and fully developed. Blood rheology is characterized using a H-B fluid model. The wall of the stenosed artery is assumed to be rigid and impermeable.

2.1 Governing equations

The cylindrical polar coordinates comprise three parameters, namely, the radial coordinate $(\overline{r})$, axial coordinate $(\overline{z})$ and the azimuthal angle, $\overline{\theta}$. Note that this study ignores the velocity of the fluid in $\overline{r}$ direction since its magnitude is negligibly small and it only considers the direction of $\overline{z}$. Therefore, $\overline{u}_{\overline{r}} = \overline{u}_{\overline{\theta}} = 0$. Moreover, the velocity $\overline{u}_{\overline{z}}$ refers to an independent and uniform in both $\overline{z}$ and $\overline{\theta}$ directions due to the axial symmetry, hence, the momentum equation of axial and radial components is reduced to the following [26, 28]:

$$\frac{d\overline{p}}{d\overline{z}} = -\frac{1}{\overline{r}}\frac{d}{d\overline{r}}(\overline{r}\overline{\tau}), \tag{1}$$

$$\frac{d\overline{p}}{d\overline{r}} = 0, \tag{2}$$

in which the constant pressure as well as shear stress, are represented as $\overline{p}$ and $\overline{\tau}$, respectively. Equation (1) deploys that the pressure differs only in the axial direction. Here, the equation given

below displays the constitutive equation of H-B fluid [34, 10]:

$$\frac{d\bar{u}}{d\bar{r}} = \begin{cases} -\frac{1}{\eta_{HB}}\left(\bar{\tau} - \bar{\tau}_y\right)^n & \text{if} \quad \bar{\tau} \geq \bar{\tau}_y, \\ 0 & \text{if} \quad \bar{\tau} < \bar{\tau}_y, \end{cases} \tag{3}$$

in which $\overline{\tau}_{\overline{y}}$ and $\overline{u}$ denote the yield stress and axial velocity, accordingly. The H-B fluid viscosity coefficient can be expressed by η_{HB} with a dimension of $\left(ML^{-1}T^{-2}\right)^n T$ whereas the power-law index is n. Equation (3) illustrates that normal shear flow takes place in the region provided that $\overline{\tau} \geq \overline{\tau}_{\overline{y}}$. On the other hand, plug flow field or solid-like fluid occurs when $\overline{\tau} < \overline{\tau}_{\overline{y}}$. Besides, Bessonov et al. [8] claimed that the fluid in the region would not flow if the yield stress were higher compared to the shear stress. Furthermore, in this area, fluid (blood) will not flow. As a solid mass is transported at a constant velocity, it is somehow transported by fluid particles found in the nearby shear flow region. The unknown parameters, shear stress $\overline{\tau}$ and velocity $\overline{u}$, can be solved by utilizing equations (1) and (3) depending on the boundary conditions expressed as follows:

$$\bar{\tau} \text{ is finite} \quad \text{at} \quad \bar{r} = 0, \tag{4}$$

$$\bar{u} = 0 \quad \text{at} \quad \bar{r} = \bar{R}(\bar{z}). \tag{5}$$

The finite yield stress effect, as seen in the boundary condition, equation (4), is that fluid exhibits a behaviour which is solid-like or plug flow (in which all velocity gradient can be negligible) in regions where the shear stress is less than the yield stress ($\overline{\tau} < \overline{\tau}_{\overline{y}}$) at $\overline{r} = 0$. However, since the fluid is viscous, it tends to sticks to the arterial wall, referred to as a no-slip condition as in equation (5) when $\overline{r} = \overline{R}\left(\overline{z}\right)$.

2.2 Non-dimensionalisation

The dimensionless variables below are introduced:

$$\begin{aligned} C &= \frac{\bar{C}}{\bar{C}_0}, \quad u = \frac{\bar{u}}{u_0}, \quad u_m = \frac{\bar{u}_m}{u_0}, \quad r = \frac{\bar{r}}{R_0}, \quad R(z) = \frac{\bar{R}(\bar{z})}{R_0}, \\ \tau &= \frac{\bar{\tau}}{(p_0 R_0/2)}, \quad \tau_y = \frac{\bar{\tau}_y}{(p_0 R_0/2)}, \quad l_0 = \frac{\bar{l}_0}{R_0}, \quad \delta = \frac{\bar{\delta}}{R_0}, \end{aligned} \tag{6}$$

where solute concentration = C, velocity = u, average velocity = u_m, stenosis height = δ, centreline velocity: $u_0 = \dfrac{R_0^{n+1} {p_0}^n}{2^n \eta_{HB}}$, the stenotic artery radius = $R\left(z\right)$, radial distance = r, shear stress = τ, yield stress = τ_y, stenosis length = l_0 and $\eta_{HB} = \mu\left(\frac{p_0 R_0}{2}\right)^{n-1}$, and μ denotes the coefficient of viscosity with regard to a Newtonian fluid.

2.3 Geometry of stenosis

The artery geometry, which is in a dimensionless form, can be expressed as follows [19]:

$$R(z) = \begin{cases} 1 - \dfrac{3\delta}{2{l_0}^4}\left[11(z-d){l_0}^3 - 47(z-d)^2{l_0}^2 + 72(z-d)^3 l_0 - 36(z-d)^4\right], & d \leq z \leq d + l_0, \\ 1, & \text{Otherwise}, \end{cases} \tag{7}$$

where the maximum stenosis height appears at $d + l_0/3$ as well as $d + 2l_0/3$, the distance with regard to the stenosis from the inlet = d, while the artery's length = L. Here, the geometry with regard to an artery with overlapping stenosis under consideration is displayed in Figure 1.

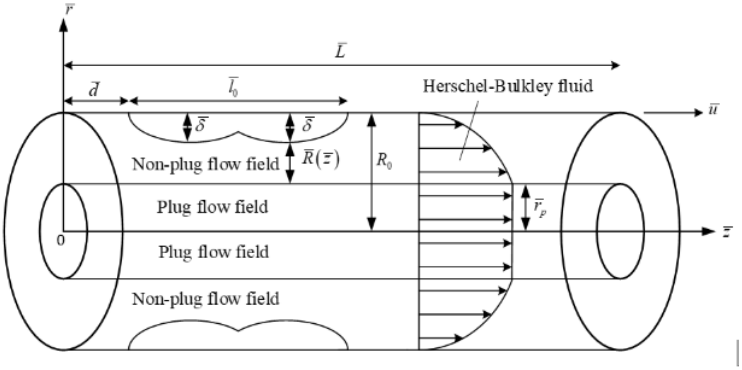

Figure 1: The geometry of an overlapping stenosed artery.

2.4 Mass transport

The convection-diffusion equation [7], which is represented in equation (8), governs the mass transport flow in the bloodstream in the dimensionless form given by

$$\frac{\partial C}{\partial t} + u\frac{\partial C}{\partial z} = \left(\frac{1}{r}\frac{\partial}{\partial r}\left(r\frac{\partial}{\partial r}\right) + \frac{1}{Pe^2}\frac{\partial^2}{\partial z^2}\right)C, \tag{8}$$

where Peclet number = Pe, dispersion time = t, and coefficient of mass diffusion = D_m.

2.5 Method of solution

The equation measuring the shear stress is achieved by integrating equation (1) to r under boundary condition (4) and is written as follows:

$$\bar{\tau} = -\frac{\bar{r}}{2}\frac{d\bar{p}}{d\bar{z}}. \tag{9}$$

The velocity of the outer as well as plug flow fields with regard to non-dimensional forms in equation (6) is generated by substituting equation (9) into equation (3), followed by integrating the result to r with the boundary condition (5), as shown below:

$$u_+(r) = \left[\frac{R(z)^{n+1}}{(n+1)} - \frac{r^{n+1}}{(n+1)} - r_p\left(R(z)^n - r^n\right) + \frac{n}{2}r_p^2\left(R(z)^{n-1} - r^{n-1}\right)\right]2^n, \tag{10}$$

$$\text{if} \quad \tau \geq \tau_y \quad \text{and} \quad r_p \leq r \leq R(z),$$

$$u_-(r_p) = \left[\frac{R(z)^{n+1}}{(n+1)} - r_p R(z)^n + \frac{n}{2}{r_p}^2 R(z)^{n-1} - \frac{n(n-1)}{2(n+1)}{r_p}^{n+1}\right]2^n, \tag{11}$$

$$\text{if} \quad \tau < \tau_y \quad \text{and} \quad 0 \leq r < r_p.$$

As per Gill and Sankarasubramanian [16], the solution to equation (8) is measured as a series expansion and depicted as:

$$C(r,z,t) = C_m(z_1,t) + \sum_{i=R(z)}^{\infty} f_i(r,t)\frac{\partial^i C_m(z_1,t)}{\partial z_1^i}, \tag{12}$$

in which dispersion function = f_i, mean concentration = C_m, while a new axial coordinate moving with the average velocity is $z_1 = z - u_m t$. Additionally, as time starts, C_m distribution is diffusive. Hence, the GDM as appropriate functions of time t can be written as follows:

$$\frac{\partial C_m}{\partial t} = \sum_{i=1}^{\infty} K_i\,(t)\,\frac{\partial^i C_m}{\partial z_1^i}\,(z_1, t)\,, \tag{13}$$

where $K_i\,(t)$ resembles the dispersion coefficient. The series expansion is obtained by employing equation (13) and substituting equation (12) in equation (8). The function of f_1 in Eq. (12) is the most essential to measure C. By equating the coefficients of $\partial^i C_m/\partial z_1^i$ and let $f_1\,(r,t) = f_{1s}\,(r) + f_{1t}\,(r,t)$, in which f_{1s} refers to the steady-state while f_{1t} represents the state which is unsteady. Here, the variable separation method as well as the Bessel function is employed in solving the transient state, $f_{1t}\,(r,t)$ of the dispersion function provided that $f_{1t}\,(r,0) = -f_{1s}\,(r)$ and $\partial f_{1t}/\partial r = 0$. The solution $f_{1t}\,(r,t)$ is numerically computed by employing Simpson's 3/8 rule expressed as:

$$f_{1t}\,(r,t) = \sum_{m=1}^{\infty} A_m\; e^{-\lambda_m^2 t}\; J_0\,(\lambda_m\; r)\,, \tag{14}$$

where,

$$A_m = -\frac{\int_0^{R(z)} J_0\,(\lambda_m\; r)\;\; f_{1s}\,(r)\, r\; dr}{\int_0^{R(z)} J_0^2\,(\lambda_m\; r)\;\; r\; dr} = -\frac{2}{J_0^2\,(\lambda_m)}\int_0^{R(z)} J_0\,(\lambda_m\; r)\;\; f_{1s}\,(r)\, r\; dr. \tag{15}$$

Here, eigenvalues λ_m represent the roots of the equation $J_1\,(r) = 0$. Moreover, J_0 and J_1 represents Bessel functions of the first kind of order zero and one, accordingly. Additionally, the dispersion coefficient of the solute $K_2\,(t)$ is obtained by substituting equations (10), (11), and the solution of $f_1\,(r,t)$, which is displayed as follows:

$$K_2\,(t) = \frac{1}{Pe^2} - 2\int_0^{R(z)} f_1\; u\; r\; dr. \tag{16}$$

The terms $K_3\,(t)$ and higher-order terms are ignored since the value is negligibly small. Thus, equation (13) is simplified to:

$$\frac{\partial C_m}{\partial t} = K_2\,(t)\,\frac{\partial^2 C_m}{\partial z_1^2}\,(z_1, t)\,. \tag{17}$$

The following equations show the boundary and initial conditions for $C_m\,(z_1, t)$:

$$C_m\,(z_1, 0) = \begin{cases} 1, & \text{if} \quad |z_1| \le \dfrac{z_s}{2}, \\ 0, & \text{if} \quad |z_1| > \dfrac{z_s}{2}, \end{cases} \tag{18}$$

and

$$C_m\,(\infty, t) = 0. \tag{19}$$

The linear second-order partial differential equation of equation (17), with the help of conditions (18) and (19), is transformed into a linear ordinary differential equation analytically using the Fourier transform, the inverse Fourier transform, and the convolution theorem to obtain the C_m as presented below:

$$C_m\,(z_1, t) = \frac{1}{2}\left[\operatorname{erf}\left(\frac{z_s/2 - z_1}{2\sqrt{\xi}}\right) + \operatorname{erf}\left(\frac{z_s/2 + z_1}{2\sqrt{\xi}}\right)\right], \tag{20}$$

where,

$$\xi\,(t) = \int_0^t K_2\,(s)\, ds. \tag{21}$$

By substituting $C_m\,(z_1, t)$ and $f_1\,(r,t)$ into equation (12) and ignoring the higher-order terms, the local concentration $C\,(r, z_1, t)$ is obtained as shown below:

$$C\,(r, z_1, t) = C_m\,(z_1, t) + f_1\,(r,t)\,\frac{\partial C_m\,(z_1, t)}{\partial z_1}. \tag{22}$$

3 Results and Discussion

The aim of the study was to assess the blood flow behaviour in the presence of stenosis and also to examine the non-Newtonian rheological behaviour by varying the physical parameters. The effect of varying slug input lengths z_s, the power-law index n, the yield stress r_p, as well as stenosis height δ with respect to the mean concentration of the solute C_m has been employed, with a range of parameters values: $r_p : 0 - 0.3$, $\delta : 0 - 0.04$, $n : 0.5 - 1.5$, and $z_s : 0.004 - 0.019$ [7, 26]. Mathematica software was employed to create data and results for comparison and validation purposes. The results of Gill and Sankarasubramanian [16] were equivalent to the mean concentration of solute obtained in our investigation, according to Figures 2(a) and 2(b). For validation purposes, the value of r_p was set to zero while the geometry of the stenosed artery, $R(z)$ as well as n was fixed to one to portray the Newtonian fluid without stenosis as presented in [16].

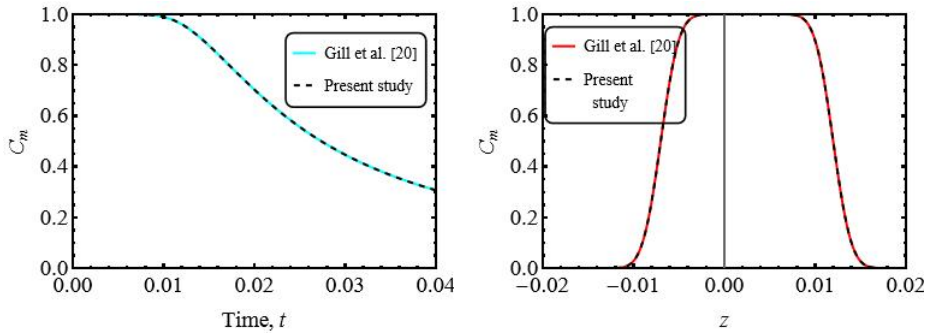

Figure 2: Validation of the mean concentration of solute (a) with time, t (b) with axial distance, z.

Figure 3(a) depicts the variation in the mean concentration of solute with time for the different slug inputs of solute length z_s when $z = 0.5$, $r_p = 0.1$, $n = 0.95$, $l_0 = 3$, $d = 2$, $\delta = 0.01$ and $Pe = 1000$. It can be seen that the peak of the mean concentration C_m occurs at t = 1.15 for various slug input lengths. Moreover, the peak of C_m ascends with the raise of slug input length z_s. Furthermore, there is a two-fold increase when z_s increases from 0.004 to 0.008. A four-fold increase can be seen when $z_s = 0.019$. Here, the mean concentration of solute is seen to increase slowly with time which then reaches the peak position (higher concentration) in a natural way. The mean concentration of solute then decreases and finally disappears. The molecular diffusion caused by the concentration gradient from an area with high concentration to a region of low concentration increases the solute's mean concentration.

The variation in mean solute concentration over time for various fluids is shown in Figure 3(b). Based on the blood's rheology, it is noticed that the peak of mean concentration C_m is greater for the non-Newtonian nature ($r_p > 0$) of the blood compared to the Newtonian nature ($r_p = 0$). These results are in line with findings from Roy and Shaw's [26]. The peak of C_m for Newtonian fluid occurs at $t = 0.98$, for Bingham fluid when $r_p = 0.1$, $n = 1$ is at $t = 1.1$. Additionally, in the case of Power-law fluid when $r_p = 0$, $n = 0.5$, the peak of C_m is reached at $t = 1.13$ and for H-B fluid when $r_p = 0.1$, $n = 0.5$ is at $t = 1.25$. More drug particles swiftly reach the disease site as the mean concentration rises by increasing the number of particles capable of getting there. It is generally known that the power-law index and yield stress boost the mean solute concentration, which improves the target disease recovery rate.

Figure 3(c) demonstrates how the mean solute concentration changes over time for different stenosis heights δ when $z_s = 0.019$, $z = 0.5$, $r_p = 0.1$, $n = 0.95$, $l_0 = 3$, $d = 2$ and $Pe = 1000$. The peak of C_m escalates when there is a rise in the stenosis height at $t = 1.12$. These findings show that as the stenosis height increases considerably, the radius of the stenotic artery decreases from $R(z) = 1, 0.99, 0.98, 0.97$ to 0.96, making the arterial wall narrower because of the accumulation of fats, lipids, cholesterols, as well as other unwanted substances found at the arterial wall. As a result, the normal flow of blood in the artery wall

is disrupted. Both blood flow and the magnitude of the flow rely on the height of the stenosis [5]. Misra and Chakravarty [21] found that improvement in stenosis height will decrease the amount of blood hematocrit in the stenotic area, resulting in reduced blood viscosity.

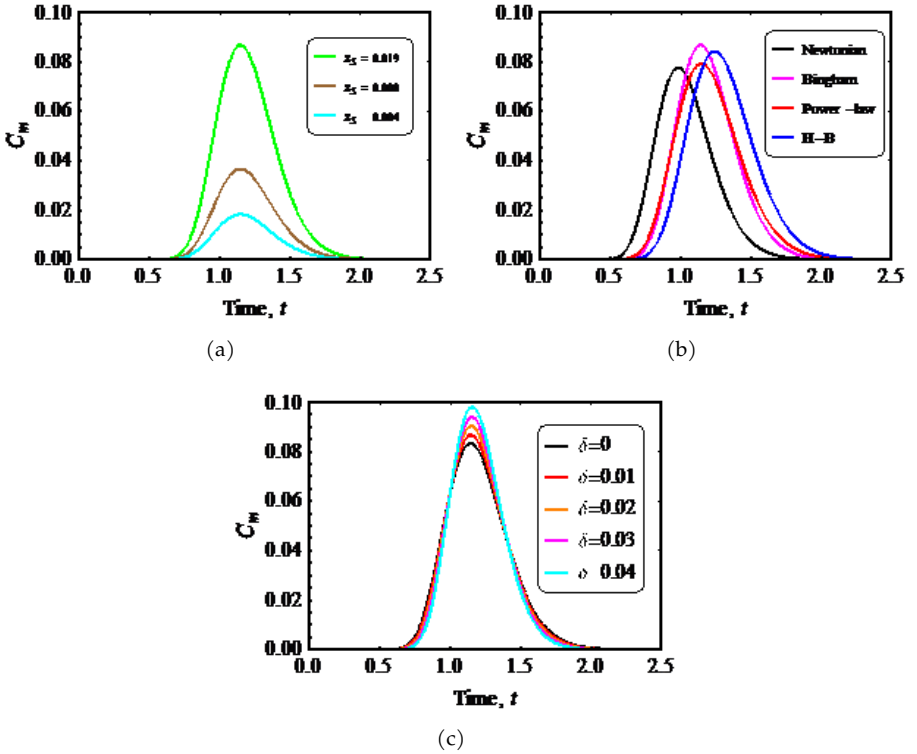

Figure 3: Variation of the mean concentration of the solute with time for various solute length z_s (a), type of fluids (b), and (c) stenosis height δ.

Table 1 provides results of the difference in mean concentration as well as the concentration of solute with time for various yield stress. Yield stress relates to the non-Newtonian nature of the fluid, and when increasing the yield stress, the viscosity of the blood tends to increase as well. At the same moment, the yield stress is related to the radius of the plug region by the relation $\tau_y = r_p/2$, which illustrates that the radius of the plug region rises when there is an increase in the yield stress. It can be seen that with a rise in the plug core radius or yield stress, the flow velocity decreases, and hence the mean concentration and concentration of solute also increases. Moreover, the peak of the mean concentration C_m and concentration of solute C occurs at different t as r_p is varied.

Table 2 illustrates the results of the difference in mean concentration as well as the concentration of solute with axial distance for various power-law indexes. Power-law index is crucial in controlling the viscosity as well as the velocity of a fluid. When the power-law index escalates from $n = 0.5, 1$ to 1.5, the viscosity of fluid also rises, thus reducing the mean concentration and concentration of solute. Furthermore, the peak mean concentration C_m and concentration of solute C occurs at $z = 0.04$ when $n = 0.5$ and 1, whereas when $n = 1.5$, it is at $z = 0.05$. As n increases, the shear thinning nature of the fluid reduces. Consequently, both flow velocity as well as dispersion coefficient decreases. Hence, the mean concentration C_m and concentration of solute C rises.

Table 1: Variation of mean concentration and concentration of solute with time for different plug core radius.

Time, t	C_m			C		
	$r_p = 0.1$	$r_p = 0.2$	$r_p = 0.3$	$r_p = 0.1$	$r_p = 0.2$	$r_p = 0.3$
1.3	0.06675	0.06797	0.07406	0.06680	0.06794	0.07399
1.4	0.04490	0.06810	0.08628	0.04498	0.06811	0.08623
1.5	0.02636	0.07808	0.09263	0.02645	0.07812	0.09259
1.6	0.01386	0.05353	0.11453	0.01396	0.05359	0.11452
1.7	0.00665	0.03191	0.11186	0.00675	0.03198	0.11187

Table 2: Variation of mean concentration and concentration of solute with axial distance for different power-law index.

z	C_m			C		
	$n = 0.5$	$n = 1$	$n = 1.5$	$n = 0.5$	$n = 1$	$n = 1.5$
0.00	0.07488	0.05878	0.05733	0.07494	0.05883	0.05739
0.01	0.14361	0.11809	0.11128	0.14366	0.11814	0.11133
0.02	0.22819	0.19764	0.18302	0.22823	0.19769	0.18306
0.03	0.30056	0.27564	0.25513	0.30058	0.27567	0.25516
0.04	0.32823	0.32040	0.30150	0.32822	0.32041	0.30151
0.05	0.29719	0.31046	0.30208	0.29717	0.31044	0.30207

4 Conclusions

The current research aimed to investigate how the height of the stenosis and non-Newtonian behaviour affected the solute dispersion in the cardiovascular system. Additionally, the following is an overview of the primary results:

1. Mean concentration and concentration of solute are improved with a rise in the slug input length, power-law index, yield stress, as well as stenosis height;
2. The peak C_m demonstrates the maximum concentration and effective concentration, whereas the maximum C_m is the effective dose for therapeutic concentration. The side effects of a specific drug can be predicted by determining the maximum concentration;
3. When the solute disperses in the H-B fluid model, the mean solute concentration is considerably greater. The H-B fluid's yield stress as well as the power-law index make it possible to control the fluid's viscosity. The H-B fluid model, therefore, provides a more precise model of blood rheology.

It is believed that this analysis would provide valuable insight into CVD and aid researchers in their knowledge of solute diffusion and solute dispersion in blood flow. Additionally, by determining the drug's concentration in the arteries' bloodstream, researchers can predict the appropriate dose for therapeutic concentration. Future study may applies and compares these research findings with the experimental results. From this research, scientists, pharmaceutical companies, and drug production companies (drug industries) can create more effective medications for medical use by observing the drug concentration and blood flow behaviour.

The primary focus of this study is on the solute concentration in the dispersion process in a steady flow. Further investigation into the effects of flow pulsatility on fluid dispersion in stenosis will be helpful, given that blood flow is highly pulsatile in nature. Additionally, this study is limited strictly to mathematical analysis. The results might be more significant and generously add to the experiment's observations. In order to enhance the study, additional experimental findings related to the dispersion of a solute in blood flow with stenosis are advised for future research.

Acknowledgement The authors would like to express their gratitude to all anonymous reviewers for their valuable feedback and suggestions, which greatly contributed to the improvement of this paper.

Conflicts of Interest The authors declare no conflict of interest.

References

[1] Z. Abbas, A. Shakeel, M. Rafiq, S. Khaliq, J. Hasnain & A. Nadeem (2022). Rheology of peristaltic flow in couple stress fluid in an inclined tube: Heat and mass transfer analysis. *Advances in Mechanical Engineering*, *14*(11), 16878132221139984. https://doi.org/10.1177/16878132221139984.

[2] S. N. A. M. Z. Abidin, N. A. Jaafar & Z. Ismail (2022). Herschel-Bulkley model of blood flow through an asymmetric stenosed artery on unsteady reactive solute dispersion. *MATEMATIKA: Malaysian Journal of Industrial and Applied Mathematics*, *38*(1), 1–20.

[3] R. D. Alsemiry, P. K. Sarifuddin, H. M. Sayed & N. Amin (2020). Effects of pulsatility and double stenoses on power law model of blood flow and mass transport in vessel. *Journal of Heat and Mass Transfer*, *19*(1), 97–128. https://doi.org/10.17654/HM019010097.

[4] R. Aris (1956). On the dispersion of a solute in a fluid flowing through a tube. In *Proceedings of the Royal Society of London. Series A. Mathematical and Physical Sciences*, volume 235 pp. 67–77. The Royal Society London,. https://doi.org/10.1098/rspa.1956.0065.

[5] K. N. Asha & N. Srivastava (2021). Geometry of stenosis and its effects on the blood flow through an artery-A theoretical study. In *AIP Conference Proceedings*, volume 2375. AIP Publishing. https://doi.org/10.1063/5.0066510.

[6] A. Ausaru & P. Nagarani (2022). Effect of external body acceleration on solute dispersion in unsteady non-newtonian fluid flow-the generalized dispersion model approach. *International Journal of Applied and Computational Mathematics*, *8*(13), 1–21. https://doi.org/10.1007/s40819-021-01209-w.

[7] O. A. Beg, S. Debnath & A. K. Roy (2022). Reactive solute transport in blood flow through a permeable capillary. *Archives of Mechanics*, *74*(2–3), 173–200. http://doi.org/10.24423/aom.3955.

[8] N. Bessonov, A. Sequeira, S. Simakov, Y. Vassilevskii & V. Volpert (2016). Methods of blood flow modelling. *Mathematical Modelling of Natural Phenomena*, *11*(1), 1–25. https://doi.org/10.1051/mmnp/201611101.

[9] V. Carvalho, D. Pinho, R. A. Lima, J. C. Teixeira & S. Teixeira (2021). Blood flow modeling in coronary arteries: A review. *Fluids*, *6*(2), 53. https://doi.org/10.3390/fluids6020053.

[10] S. S. Chauhan & A. Tiwari (2022). Solute dispersion in non-newtonian fluids flow through small blood vessels: A varying viscosity approach. *European Journal of Mechanics-B/Fluids*, *94*, 200–211. https://doi.org/10.1016/j.euromechflu.2022.02.009.

[11] M. S. Dada, A. J. Babatunde & M. M. Tunde (2022). Fluid analysis of double-layered blood flow through a tapered overlapping stenosed artery with a porous wall. *Journal of Heat and Mass Transfer Research*, *9*(2), 189–196.

[12] N. Dash & S. Singh (2020). Analytical study of non-Newtonian Reiner–Rivlin model for blood flow through tapered stenotic artery. *Mathematical Biology and Bioinformatics*, *15*(2), 295–312. https://doi.org/10.17537/2020.15.295.

[13] M. A. El Kot & Y. Abd Elmaboud (2023). Model of LDL-C concentration of blood flow through a vertical porous microchannel with multiple stenoses: computational simulation. *Journal of Taibah University for Science*, *17*(1), 2176194. https://doi.org/10.1080/16583655.2023.2176194.

[14] N. Freidoonimehr, R. Chin, A. Zander & M. Arjomandi (2020). An experimental model for pressure drop evaluation in a stenosed coronary artery. *Physics of Fluids*, *32*(2). https://doi.org/10.1063/1.5139701.

[15] S. Gajbhiye, A. Warke & K. Ramesh (2022). Analysis of energy and momentum transport for casson nanofluid in a microchannel with radiation and chemical reaction effects. *Waves in Random and Complex Media*, pp. 1–29. https://doi.org/10.1080/17455030.2022.2097749.

[16] W. Gill & R. Sankarasubramanian (1970). Exact analysis of unsteady convective diffusion. In *Proceedings of the Royal Society of London. A. Mathematical and Physical Sciences*, volume 316 pp. 341–350. The Royal Society London,. https://doi.org/10.1098/rspa.1970.0083.

[17] K. E. Hossain & M. M. Haque (2017). Influence of magnetic field on chemically reactive blood flow through stenosed bifurcated arteries. In *AIP Conference Proceedings*, volume 1851. AIP Publishing. https://doi.org/10.1063/1.4984641.

[18] A. Hussain, L. Sarwar, A. Rehman, Q. Al Mdallal, A. H. Almaliki & A. El-Shafay (2022). Mathematical analysis of hybrid mediated blood flow in stenosis narrow arteries. *Scientific Reports*, *12*(1), 12704. https://doi.org/10.1038/s41598-022-15117-6.

[19] G. Layek, S. Mukhopadhyay & R. S. R. Gorla (2009). Unsteady viscous flow with variable viscosity in a vascular tube with an overlapping constriction. *International Journal of Engineering Science*, *47*(5-6), 649–659. https://doi.org/10.1016/j.ijengsci.2009.01.011.

[20] K. S. Mekheimer, R. Abo-Elkhair, S. I. Abdelsalam, K. K. Ali & A. Moawad (2022). Biomedical simulations of nanoparticles drug delivery to blood hemodynamics in diseased organs: Synovitis problem. *International Communications in Heat and Mass Transfer*, *130*, 105756. https://doi.org/10.1016/j.icheatmasstransfer.2021.105756.

[21] J. Misra & S. Chakravarty (1986). Flow in arteries in the presence of stenosis. *Journal of Biomechanics*, *19*(11), 907–918. https://doi.org/10.1016/0021-9290(86)90186-7.

[22] S. Orizaga, D. N. Riahi & J. R. Soto (2020). Drug delivery in catheterized arterial blood flow with atherosclerosis. *Results in Applied Mathematics*, *7*, 100117. https://doi.org/10.1016/j.rinam.2020.100117.

[23] B. Prashantha & S. Anish (2019). Discrete-Phase modelling of an asymmetric stenosis artery under different womersley numbers. *Arabian Journal for Science and Engineering*, *44*(2), 1001–1015. https://doi.org/10.1007/s13369-018-3391-z.

[24] D. N. Riahi & S. Orizaga (2023). Modeling and computation for unsteady blood flow and solute concentration in a constricted porous artery. *AIMS Bioengineering*, *10*(1), 67–88. https://doi.org/10.3934/bioeng.2023007.

[25] A. K. Roy & O. A. Bég (2021). Mathematical modelling of unsteady solute dispersion in two-fluid (micropolar-newtonian) blood flow with bulk reaction. *International Communications in Heat and Mass Transfer*, *122*, 105169. https://doi.org/10.1016/j.icheatmasstransfer.2021.105169.

[26] A. K. Roy & S. Shaw (2021). Shear augmented microvascular solute transport with a two-phase model: Application in nanoparticle assisted drug delivery. *Physics of Fluids*, *33*(3), 031904. https://doi.org/10.1063/5.0035754.

[27] A. Saleem, S. Akhtar, S. Nadeem, A. Issakhov & M. Ghalambaz (2020). Blood flow through a catheterized artery having a mild stenosis at the wall with a blood clot at the centre. *Computer Modeling in Engineering & Sciences*, *125*(2), 565–577. https://doi.org/10.32604/cmes.2020.011883.

[28] D. Sankar, K. Viswanathan, A. K. Nagar, N. A. Binti Jaafar & A. V. Kumar (2022). Theoretical study on poiseuille flow of herschel-bulkley fluid in porous media. *Journal of Applied and Computational Mechanics*, *8*(4), 1246–1269.

[29] N. Santhosh, G. Radhakrishnamacharya & A. J. Chamkha (2015). Effect of slip on herschel–bulkley fluid flow through narrow tubes. *Alexandria Engineering Journal*, *54*(4), 889–896. https://doi.org/10.1016/j.aej.2015.07.009.

[30] B. K. Sharma, R. Gandhi, T. Abbas & M. Bhatti (2023). Magnetohydrodynamics hemodynamics hybrid nanofluid flow through inclined stenotic artery. *Applied Mathematics and Mechanics*, *44*(3), 459–476. https://doi.org/10.1007/s10483-023-2961-7.

[31] S. Singh & P. Murthy (2022). Unsteady solute dispersion in non-newtonian fluid flow in a tube with wall absorption-deviation from the gaussianity. *Physics of Fluids*, *34*(6), 061908. https://doi.org/10.1063/5.0096941.

[32] G. I. Taylor (1953). Dispersion of soluble matter in solvent flowing slowly through a tube. In *Proceedings of the Royal Society of London. Series A. Mathematical and Physical Sciences*, volume 219 pp. 186–203. The Royal Society London,. https://doi.org/10.1098/rspa.1953.0139.

[33] T. Tivde, A. Ochayi & M. Iorkua (2021). Mathematical modelling of arterial constriction in the presence of blood diseases. *Journal of Mobile Computing and Application*, *8*(1), 22.

[34] A. Tiwari, P. D. Shah & S. S. Chauhan (2021). Unsteady solute dispersion in two-fluid flowing through narrow tubes: A temperature-dependent viscosity approach. *International Journal of Thermal Sciences*, *161*, 106651. https://doi.org/10.1016/j.ijthermalsci.2020.106651.

[35] M. N. Uddin, M. M. Uddin & M. M. Alam (2020). Comparative mathematical study of blood flow through stenotic and aneurysmatic artery with the presence and absence of blood clots. *Malaysian Journal for Mathematical Sciences*, *16*(3), 599–623. https://doi.org/10.47836/mjms.16.3.12.

[36] S. A. Wajihah & D. Sankar (2023). A review on non-newtonian fluid models for multi-layered blood rheology in constricted arteries. *Archive of Applied Mechanics*, *93*(5), 1771–1796. https://doi.org/10.1007/s00419-023-02368-6.

[37] N. M. Zain & Z. Ismail (2023). Numerical solution of magnetohydrodynamics effects on a generalised power law fluid model of blood flow through a bifurcated artery with an overlapping shaped stenosis. *Plos One*, *18*(2), e0276576. https://doi.org/10.1371/journal.pone.0276576.